Heuristic Rule for Binary Superlattice Coassembly: Mixed Plastic Mesophases of Hard Polyhedral Nanoparticles

Mihir R. Khadilkar
Department of Physics, Cornell University, Ithaca, New York 14853, USA

Fernando A. Escobedo*
Department of Chemical and Biomolecular Engineering, Cornell University, Ithaca, New York 14853, USA

(Received 21 June 2014; published 17 October 2014)

Sought-after ordered structures of mixtures of hard anisotropic nanoparticles can often be thermodynamically unfavorable due to the components' geometric incompatibility to densely pack into regular lattices. A simple compatibilization rule is identified wherein the particle sizes are chosen such that the order-disorder transition pressures of the pure components match (and the entropies of the ordered phases are similar). Using this rule with representative polyhedra from the truncated-cube family that form pure-component plastic crystals, Monte Carlo simulations show the formation of plastic-solid solutions for all compositions and for a wide range of volume fractions.

DOI: 10.1103/PhysRevLett.113.165504 PACS numbers: 61.43.Bn, 61.46.Df, 64.75.Xc

Polyhedral colloidal nanoparticles are versatile building blocks for designing novel materials with targeted emergent properties. Recent developments in experimental techniques [1–7] to controllably synthesize and manipulate polyhedral nanoparticles have fueled many theoretical [8,9] and simulation studies [10–20] to understand their packing and phase behavior. These building blocks have been shown to exhibit a rich phase behavior at finite osmotic pressures unveiling the presence of novel mesophases. A mesophase is a partially ordered phase whose properties are intermediate between those of disordered liquids and ordered crystals, such as liquid crystals, rotator plastic crystals, and quasicrystals.

Binary mixtures of polyhedra [21] exhibit a competition between mixing and packing entropy that often leads to phase separation at high pressures; indeed, assembly into binary superlattices using just entropic forces is difficult to achieve [22]. An earlier study [21] on the miscibility trends of binary polyhedra mixtures revealed the importance of the relative size ratio of the components and of similarity in their mesophase behavior [10]. One of our aims is to identify shapes and sizes that favor the formation of entropic rotator mixtures.

A family of truncated cubes, which is readily synthesizable [3,4], has been recently shown to exhibit a diverse set of phases [12]. Further, the kinetics of the disorder-to-order transition for some members of this family has been shown to be substantially faster than that of hard spheres [23], making them appealing choices for applications requiring fast self-assembly. In addition to cuboctahedra (COs) and truncated octahedra (TOs), we choose here a truncated cube with truncation parameter 0.4 (TC4) [12], since, like COs and TOs, TC4 also exhibits a rotator mesophase [12]. These choices are motivated by the hypothesis that mesophasic partial disorder can provide enough structural leeway to facilitate ordered solutions to form despite the entropy costs associated with differences in packing. The main mixtures studied are the three possible pairings of these three shapes, and are denoted henceforth as COTO, TC4TO, and TC4CO.

For any target solid mixture, the relative component size ratio is an important determinant to control the crystal lattice spacing. A recent study [21] suggested that the solid miscibility in a binary mixture of polyhedra can be linked to the relative values of the order-disorder transition pressure or ODP. In that study [21], however, the components' ODPs were always substantially different and very limited solid miscibility was observed; hence, the questions of what happens when the ODPs matched and whether that provides optimized mesophase compatibility were left open. For the present simulations, we set the relative particle size ratios such that their ODPs are approximately equal, which coincidentally entail near-equal circumradii; namely, the ratios of circumradii are $\mathrm{CO:TO} = 1:1$ for COTO, $\mathrm{TC4:TO} = 1.01:1$ for TC4TO, and $\mathrm{TC4:CO} = 1.01:1$ for TC4CO (for TC4 we use the largest circumscribing radius). While equal circumradii is an equivalent criterion to $\Delta\mathrm{ODP} = 0$ for the main mixtures considered here, we will also use a fourth mixture of spheres and cubes to show that $\Delta\mathrm{ODP} = 0$ optimizes the overall miscibility even when equal circumradii does not.

For the main mixtures, we probed the phase behavior as a function of pressure using hard-particle Monte Carlo simulations in the isothermal-isobaric ensemble, including swap moves between the position of particles of different species [21]. We used interfacial runs to test the relative stability of the phases near a phase transition. While most simulations used equimolar mixtures, additional runs for

other compositions were used to more completely map out the phase diagram. Orientational order was analyzed by using the P_4 order parameter [24] and orientational scatter plots [25], while the translational order was probed by using Steinhardt's order parameters Q_4 and Q_6 [29] and diffraction patterns (structure factors). To further characterize positional order, we also identified the contributions of fcc, bcc, or hcp-like motifs [10] by calculating the distributions of two local bond order parameters ($\bar{q}_4$ and $\bar{q}_6$) (see details in the Supplemental Material [25]).

The COTO, TC4TO, and TC4CO mixtures exhibit a mixed rotator mesophase (MRM) in between the isotropic phase at low pressures and a phase separated state with two crystalline phases at high pressures (see Fig. 1). This MRM is stable for all compositions in all three mixtures and for a sizable range of volume fractions [25]. It is of interest to characterize such a novel MRM since the rotator phases of the pure components are distinct in both translational order and rotational disorder. For instance, after the ODP the COs and TC4s rotator phases transform into the orientationally ordered crystal via a first-order transition at the mesophase-to-crystal transition pressure [12]; in contrast, TOs transform continuously into a crystal phase [23]. Below we examine the properties of the MRM giving representative results for the COTO mixture.

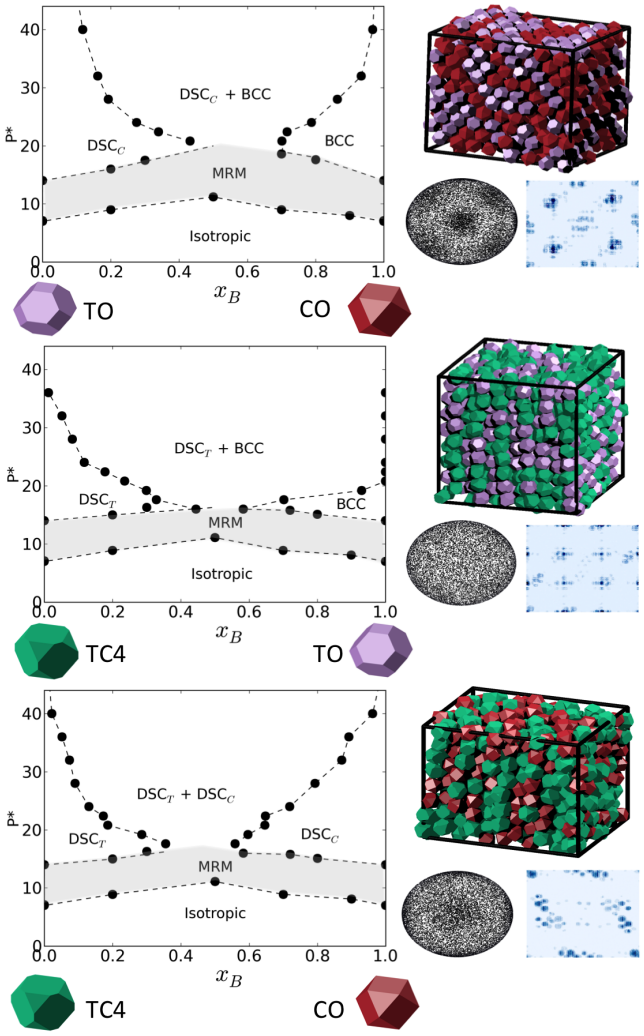

FIG. 1 (color online). Pressure (P^*) versus composition (x_B) phase diagram for the three main mixtures. DSC$_C$ and DSC$_T$ are distorted simple cubic structures of COs and TC4s, respectively [12,14]. x_B represents fraction of COs in the COTO and TC4CO mixtures, and the fraction of TOs in the TC4TO mixture. Each diagram is accompanied by a snapshot of the mixed rotator mesophase (MRM) for $x_B = 0.5$ (at $P^* = 11.2$, 9.6, and 9.6 for COTO, TC4TO, and TC4CO, respectively), its orientational correlation plot, and diffraction pattern.

In a purely entropic scenario, mixtures (that do not form tessellating compounds [22]) would be expected to phase separate at high pressures into nearly pure component solids to allow denser packings. For our ODP-matched mixtures, the MRM delays the onset of phase separation (e.g., $P^* \approx 21$ in the equimolar COTO). The observed MRM has intermediate orientational order P_4 as shown in Fig. 2(a) for the COTO mixture, and strong positional order (Q_4 and Q_6). Local compositional heterogeneity or incipient "clustering" can be detected by the average fraction of like-shaped nearest neighbors to a given particle. This fraction should equal the overall composition of the given species in the bulk for an ideal mixture, but it will exceed that as clustering and a tendency for phase separation ensues. We observe that for all three mixtures the ratio of local to global composition or "enrichment factor" f steadily increases with pressure from its ideal (well-mixed) value until eventually reaching the solid-solid phase separated state [Fig. 2(b)]. The more symmetric compositions have a larger ideal mixing entropy and hence enrichment

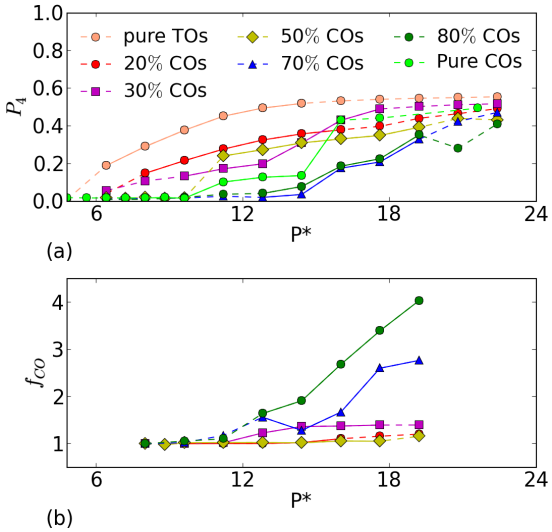

FIG. 2 (color online). Plots showing the effect of changing the mesophase composition in the COTO mixture (solid part of each curve represents the stable MRM region). (a) Variation of P_4 as a function of pressure P^*. (b) Pressure dependence of the enrichment factor.

factors closer to unity. For some of the more skewed compositions, the MRM crystallizes before phase separating as pressure increases. Figure 2(a) shows how the mesophase-to-crystal transition (as detected by the approach of P_4 to the threshold value of 0.4 for orientational order) changes from being nearly continuous for low CO compositions (similar to pure TOs) to having more abrupt increases for higher CO compositions (like pure COs [23]).

Given that none of the MRMs simulated had one of the known perfect lattice structures, we obtained the fractions of different standard structural motifs in the simulated configurations [10]. We observe that in the equimolar MRMs containing TOs (COTO and TC4TO), the fraction of bcc order (which is the target structure for TOs, the better-packing shape in the mixture) increases with volume fraction (see the Supplemental Material [25]). Similarly, for TC4CO MRM, the fraction of hcp order (which is closer to DSC_C and DSC_T structures that COs and TC4s favor, respectively) increases with volume fraction.

To test whether the equal ODP rule maximizes rotator miscibility, we use the COTO mixture as the test bed and change by $\pm 5\%$ the relative size ratio by slightly perturbing the size of the TOs from its original value (assumed unity, system O) to be 1.05 (system L, for larger TOs) and 0.95 (system S, for smaller TOs). This rescaled the ODP of the corresponding TOs from 7.1 (system O) to $7.1 \times 0.95^3 = 6.1$ (system L) and $7.1 \times 1.05^3 = 8.2$ (system S). The first observation is that systems L and S also exhibit a MRM over the whole range of compositions, showing that this MRM behavior is robust to small changes of particle size ratios (e.g., size polydispersity that may arise from the experimental synthesis). The extent of miscibility in the MRM can be quantified by using several metrics: e.g., (1) ΔP_m^*, the difference between the highest and lowest pressure where the equimolar MRM phase is stable; (2) $\Delta\phi_m$, the difference between the highest and lowest volume fraction where the equimolar MRM phase is stable; and (3) A_{MRM}, the area where the MRM exists in the volume fraction versus composition phase diagram. We observed that the extent of miscibility as inferred from all metrics decreased for systems L and S relative to system O. Further, in a previous study [21] where the size ratio was 63%, the ODP-matching value, no MRM formed for a wide range of compositions.

While the CO:TO volume ratio is not a good predictor of MRM miscibility as it is closer to unity in the L case than in the O case (see Table I), the ratio of circumradii is. Equal circumradii, which also holds for the TC4CO and TC4TO mixtures described earlier, could be envisioned as allowing two low-asphericity polyhedral components to freely rotate, effectively sweeping equal spherical volumes in the lattice sites of the MRM. This picture is too simplistic, however, since TOs do not freely rotate in their mesophase [23].

TABLE I. Summary of results for the miscibility range for the COTO mixture in the original and changed size ratios. V_l and V_s correspond to the volume of the larger and smaller particle in the mixture, respectively. E_l and E_s denote edge lengths while R_l and R_s denote circumradii.

System	ΔODP	ΔP_m^*	$\Delta\phi_m$	A_{MRM}	V_l/V_s	E_l/E_s	R_l/R_s
O	≈ 0.0	13	0.17	7.0	1.21	1.58	1.0
S	$\approx +1.1$	9.0	0.13	6.1	1.04	1.66	1.05
L	≈ -1.0	3.0	0.09	3.6	1.41	1.50	1.05

To discriminate the role on mixture phase behavior of particles with equal ODP versus particles with equal circumradius, the components should not both be round shaped but one of them have high asphericity. For contrast, we simulated mixtures of spheres and cubes. Spheres can be seen as the limiting case of a rounded polyhedra, whose fcc solid can also be taken to be a rotator if a minimal shape anisotropy is assumed [30]. Cubes can be seen as the limiting member of the truncated cube family having minimal truncation and high asphericity, whose solid phase is no longer a rotator [10]. Figure 3 shows the phase diagrams traced using a Gibbs-Duhem integration method

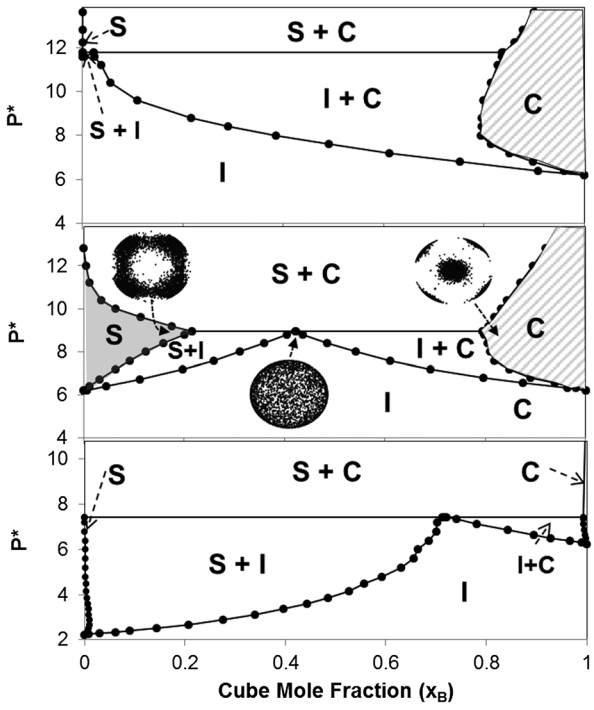

FIG. 3. Pressure-composition phase diagrams for spheres (diameter σ) and cubes (side edge d) with different size ratios. Top: $\sigma/d = 1.0$ (equal inradius). Center: $\sigma/d = 1.23$ (equal ODPs). Bottom: $\sigma/d = 1.732$ (equal circumradius). S = sphere rich solid, C = cube rich solid, I = isotropic phase. $P^* = Pd^3/\epsilon$. Data for $\sigma/d = 1.23$ are from Ref. [31]. Orientation correlation plots are shown for the cubes in the three phases occurring at the eutectic pressure.

[25,31]. Results are shown for three choices of the sphere diameter σ to cube edge d ratios: 1 (equal inradius), 1.23 (equal ODPs), and 1.732 (equal circumradius). Equal circumradii lead to minimal mutual solid solubility and an almost nonexistent MRM region. In contrast, equal ODPs lead to maximized mutual solid miscibility with both a large region where spheres dissolve in the cube-rich solid (C region) and a large MRM region where cubes dissolve in the sphere-rich solid (S region in gray). In that latter MRM, the orientation scatter plot (Fig. 3) reveals that cubes form a restricted rotator where they lack orientational order but cannot adopt certain orientations. Such orientational correlations (e.g., see Fig. 1) depend on the shape and size of the particle relative to those of the cage where it rattles [23].

The above analysis suggests that the ODP is a more generally predictive parameter of solid-phase miscibility of two shapes (beyond rotator mesophases). The ODP can be seen as marking the turning point where packing entropy takes over as the dominant entropic force determining the structure of the system. Accordingly, if the components have the same ODP, their tendencies to order will be comparable (i.e., synchronized) at any pressure above this ODP. In Fig. 1, the components have synchronized their rotator mesophases along the scale of the thermodynamic field driving the phase transitions (i.e., pressure). Indeed, for $A + B$ mixtures, if $\mathrm{ODP}_A \ll \mathrm{ODP}_B$ then for $\mathrm{ODP}_A < P < \mathrm{ODP}_B$ particles B will have a strong preference for the isotropic state, while for $P > \mathrm{ODP}_B$ where both favor ordered states, particles A would be much more compressed than those of B and prone to form a separate A-rich dense solid. If one considers the pure components and that $\mu^* = \int_0^{\mathrm{ODP}} (Z-1)/P dP$ is the residual chemical potential of the isotropic phase in coexistence with the ordered phase (Z is the compressibility factor), then for hard-core systems whose isotropic branches of the equation of state are similar (see Fig. 1 in the Supplemental Material [25]), having equal ODPs translates into pure mesophases that at the same pressure also have comparable chemical potentials and (neglecting the typically small ΔPV terms) similar entropies. If rotational entropies are also comparable (as in rotator phases), equality of ODPs then approximately translates into pure mesophases of A and B where each particle experiences a similar packing entropy or free volume: a likely helpful condition for coassembly.

As a final test of the equal-ODP rule, we simulated a ternary equimolar mixture of COs, TC4s, and TOs at ODP-matching ratios, and found that the ternary MRM is also stable (with $\Delta P_m^* \approx 3.6$; see the Supplemental Material [25]). Of course, equality of ODPs is not sufficient to ensure high solid-phase compatibility; similarity in the type of ordered structure is also important as with the rotator mesophase in the COs, TC4s, and TOs. In this context, the sphere-cube system provides a counterexample where solid miscibility over all compositions is precluded by the different pure-component solid behavior.

Recent work from Van Anders *et al.* [32,33] described the assembly of anisotropic particles as driven by an entropic bonding arising from "patches" that is quantifiable via a potential of mean force and torque (PMFT) (akin to enthalpic interactions). As the MRM is compressed and the patches get closer, any PMFT difference between like and dislike particles becomes more accentuated, making the mixed state less entropically favorable. This effect is connected with the changes in local composition discussed before regarding Fig. 2(b): like-particle contacts are favored with increasing density as though an effective attraction (repulsion) acts between the like (unlike) particle types. Eventually, the entropic cost at higher densities overpowers the mixing entropy leading to phase separation into two solids (this analysis does not apply to tessellating polyhedral compounds [22]).

Beyond polyhedral particles, binary mixtures of rigid rods (of diameters D_1 and D_2 and lengths L_1 and L_2) with ODPs associated with isotropic-nematic transitions provide further insights. Simulation [34] and Onsager's theory [35] have shown that rods sufficiently dissimilar in length and/or diameter phase separate into two nematic phases at high pressures (a sign of incompatibility). However, "symmetric" mixtures [36] where $L_2/L_1 = (D_2/D_1)^{-(1/2)}$ so that pure components have the same excluded volume, and hence identical ODPs, tend to lie well inside the predicted one-nematic phase domain (see Fig. 3 of Ref. [35]), with equimolar mixtures having components with the same extent of orientational order (a sign of maximal compatibility) and ordering at pressures below the pure-component ODPs [36]. Further, novel biaxial nematic phases have also been predicted for equal-ODP (symmetric) blends of rodlike and platelike ellipsoids [37–39]. Note that in these examples and our simulated systems, ODP equality is not a prescription that guarantees full mesophase miscibility (which could only happen when particle shapes and pure-component behaviors are not too disparate); instead, it provides a guideline for conditions that favor miscibility (even if only a partial one, as for the cube-sphere example of Fig. 3).

In summary, we find that by choosing size ratios that synchronize the onset of the plastic crystals in the pure components of a mixture, fully mixed mesophases are favored despite incompatibilities in the lattice structure of the pure component crystals. A vast array of applications [40–45] will benefit from new routes to create nanoparticle superstructures. Just as liquid-crystal phases have found widespread applications as switches and sensors, rotator phases may also find applications involving the external control of their rotational state. Since components can have different chemistries, the ability to produce rotator phases of any composition should add to this potential.

This work was supported by the U.S. National Science Foundation, Grant No. CBET 1402117. The authors also thank Dr. U. Agarwal for useful exchanges.

*fe13@cornell.edu

[1] J. Henzie, M. Grünwald, A. Widmer-Cooper, P. L. Geissler, and P. Yang, Nat. Mater. **11**, 131 (2012).

[2] W. H. Evers, B. Goris, S. Bals, M. Casavola, J. de Graaf, R. v. Roij, M. Dijkstra, and D. Vanmaekelbergh, Nano Lett. **13**, 2317 (2013).

[3] D. Seo, J. C. Park, and H. Song, J. Am. Chem. Soc. **128**, 14863 (2006)

[4] O. C. Compton and F. E. Osterloh, J. Am. Chem. Soc. **129**, 7793 (2007).

[5] W. Niu, L. Zhang, and G. Xu, ACS Nano **4**, 1987 (2010).

[6] N. V. Long, M. Ohtaki, M. Uchida, R. Jalem, H. Hirata, N. D. Chien, and M. Nogami, J. Colloid Interface Sci. **359**, 339 (2011).

[7] E. V. Shevchenko, D. V. Talapin, N. A. Kotov, S. O'Brien, and C. B. Murray, Nature (London) **439**, 55 (2006).

[8] R. Gabbrielli, Y. Jiao, and S. Torquato, Phys. Rev. E **86**, 041141 (2012).

[9] J. H. Conway, Y. Jiao, and S. Torquato, Proc. Natl. Acad. Sci. U.S.A. **108**, 11009 (2011).

[10] U. Agarwal and F. A. Escobedo, Nat. Mater. **10**, 230 (2011).

[11] F. Smallenburg, L. Filion, M. Marechal, and M. Dijkstra, Proc. Natl. Acad. Sci. U.S.A. **109**, 17886 (2012).

[12] A. P. Gantapara, J. de Graaf, R. van Roij, and M. Dijkstra, Phys. Rev. Lett. **111**, 015501 (2013).

[13] S. Torquato and Y. Jiao, Nature (London) **460**, 876 (2009).

[14] S. Torquato and Y. Jiao, Phys. Rev. E **80**, 041104 (2009).

[15] Y. Jiao, F. H. Stillinger, and S. Torquato, Phys. Rev. E **79**, 041309 (2009).

[16] M. Marechal and H. Löwen, Phys. Rev. Lett. **110**, 137801 (2013).

[17] P. F. Damasceno, M. Engel, and S. C. Glotzer, ACS Nano **6**, 609 (2012).

[18] P. F. Damasceno, M. Engel, and S. C. Glotzer, Science **337**, 453 (2012).

[19] A. Haji-Akbari, M. Engel, and S. C. Glotzer, J. Chem. Phys. **135**, 194101 (2011).

[20] U. Agarwal and F. A. Escobedo, J. Chem. Phys. **137**, 024905 (2012).

[21] M. R. Khadilkar, U. Agarwal, and F. A. Escobedo, Soft Matter **9**, 11557 (2013).

[22] M. R. Khadilkar and F. A. Escobedo, J. Chem. Phys. **137**, 194907 (2012).

[23] V. Thapar and F. A. Escobedo, Phys. Rev. Lett. **112**, 048301 (2014).

[24] B. S. John, C. Juhlin, and F. A. Escobedo, J. Chem. Phys. **128**, 044909 (2008).

[25] See Supplemental Material at http://link.aps.org/supplemental/10.1103/PhysRevLett.113.165504, which also includes Refs. [26–28], for additional details on the systems, equations of state, and order parameter analyses.

[26] N. F. Carnahan and K. E. Starling, J. Chem. Phys. **51**, 635 (1969).

[27] E. G. Golshtein and N. V. Tretyakov, *Modified Lagrangians and Monotone Maps in Optimization* (Wiley, New York, 1996).

[28] W. Lechner and C. Dellago, J. Chem. Phys. **129**, 114707 (2008).

[29] P. J. Steinhardt, D. R. Nelson, and M. Ronchetti, Phys. Rev. B **28**, 784 (1983).

[30] P. Bolhuis and D. Frenkel, J. Chem. Phys. **106**, 666 (1997).

[31] F. A. Escobedo, J. Chem. Phys. **140**, 094102 (2014).

[32] G. van Anders, N. Khalid Ahmed, D. Klotsa, M. Engel, and S. Glotzer, arXiv:1309.1187.

[33] G. van Anders, N. K. Ahmed, R. Smith, M. Engel, and S. C. Glotzer, ACS Nano **8**, 931 (2014).

[34] M. Dijkstra and R. van Roij, Phys. Rev. E **56**, 5594 (1997).

[35] P. C. Hemmer, Mol. Phys. **96**, 1153 (1999).

[36] R. P. Sear and B. M. Mulder, J. Chem. Phys. **105**, 7727 (1996).

[37] P. Camp and M. Allen, Physica (Amsterdam) **229A**, 410 (1996).

[38] P. Camp, M. Allen, P. Bolhuis, and D. Frenkel, J. Chem. Phys. **106**, 9270 (1997).

[39] S. Varga, A. Galindo, and G. Jackson, J. Chem. Phys. **117**, 10412 (2002).

[40] V. L. Colvin, MRS Bull. **26**, 637 (2001).

[41] W. U. Huynh, J. J. Dittmer, and A. P. Alivisatos, Science **295**, 2425 (2002).

[42] I. Gur, N. A. Fromer, M. L. Geier, and A. P. Alivisatos, Science **310**, 462 (2005).

[43] K. S. Leschkies, T. J. Beatty, M. S. Kang, D. J. Norris, and E. S. Aydil, ACS Nano **3**, 3638 (2009).

[44] Y.-F. Lim, J. J. Choi, and T. Hanrath, J. Nanomater. **2012**, 1 (2012).

[45] G. von Freymann, A. Ledermann, M. Thiel, I. Staude, S. Essig, K. R. Busch, and M. Wegener, Adv. Funct. Mater. **20**, 1038 (2010).